

Liquid: Language Models are Scalable Multi-modal Generators

Junfeng Wu^{1,2}, Yi Jiang^{2,†}, Chuofan Ma^{2,3},
 Yuliang Liu¹, Hengshuang Zhao³, Zehuan Yuan², Song Bai^{2,*}, Xiang Bai^{1,*}

¹Huazhong University of Science and Technology ²Bytedance Inc

³The University of Hong Kong

wjf5203@gmail.com, jiangyi.enjoy@bytedance.com,

b20mcf@connect.hku.hk, ylliu@hust.edu.cn, hszhao@cs.hku.hk

yuanzehuan@bytedance.com, songbai.site@gmail.com, xbai@hust.edu.cn

Abstract

We present Liquid, an auto-regressive generation paradigm that seamlessly integrates visual comprehension and generation by tokenizing images into discrete codes and learning these code embeddings alongside text tokens within a shared feature space for both vision and language. Unlike previous multimodal large language model (MLLM), Liquid achieves this integration using a single large language model (LLM), eliminating the need for external pretrained visual embeddings such as CLIP. For the first time, Liquid uncovers a scaling law that performance drop unavoidably brought by the unified training of visual and language tasks diminishes as the model size increases. Furthermore, the unified token space enables visual generation and comprehension tasks to mutually enhance each other, effectively removing the typical interference seen in earlier models. We show that existing LLMs can serve as strong foundations for Liquid, saving 100 \times in training costs while outperforming Chameleon in multimodal capabilities and maintaining language performance comparable to mainstream LLMs like LLAMA2. Liquid also outperforms models like SD v2.1 and SD-XL (FID of 5.47 on MJHQ-30K), excelling in both vision-language and text-only tasks. This work demonstrates that LLMs such as Qwen2.5 and GEMMA2 are powerful multimodal generators, offering a scalable solution for enhancing both vision-language understanding and generation. The code and models will be released at <https://github.com/FoundationVision/Liquid>.

1 Introduction

The recent advancement of Large Language Models (LLMs) [4, 64, 8, 48, 65, 61] has sparked a trend of extending the foundational capabilities of LLMs to the visual domain, giving rise to Multi-modal Large Language Models (MLLMs) [39, 77, 37, 42, 5, 38]. In the realm of visual understanding, MLLMs such as LLaVA [39] typically adopt the pretrained CLIP [46] model as the visual tokenizer, followed by a two-stage training process to align the vision-and-language feature space. While for text-guided visual generation, most MLLMs [18, 19, 25, 59, 58] rely on an external diffusion model to generate images. Despite these methods have achieved remarkable multi-modal understanding and generation performances, the use of external visual modules introduces additional architecture complexity to the system, and potentially poses a bottleneck when scaling up the LLMs.

*Corresponding authors: <xbai@hust.edu.cn>, <songbai.site@gmail.com>; †: project lead

In light of the aforementioned issues, an emerging line of research [15, 50, 12, 72, 63, 57] attempts to employ the VQVAE [66, 15] model as a universal visual tokenizer for MLLMs. Analogous to the role played by the BPE [54] tokenizer in LLMs, VQVAE establishes a bi-directional mapping between raw pixels and discrete codes. This enables the MLLMs to learn visual code embeddings jointly with text tokens, rather than constrained by the feature space of a pretrained visual encoders like CLIP or pretrained visual generators like diffusion models. Moreover, the discrete nature of visual tokens allows uniform modeling of visual and text tokens with the same next-token prediction loss, which seamlessly integrates both modalities. LWM [40] and Chameleon [60] are the pioneers in exploring this approach. However, these methods involve extensive training from scratch, which makes it computationally expensive to disseminate exploration in this form. Follow-up works further introduces bi-directional attention [76], discrete diffusion modeling [71], and residual codes [70] to handle visual tokens. EMU3 [67] has verified that the next prediction paradigm can achieve SOTA results in both understanding and generation tasks by finetuning separate two models, but there is a lack of exploration of the effects of unifying these two tasks within one model. In this paper, we explore the potential of solely employing LLMs as multimodal generators, and conduct a comprehensive empirical study to investigate a series of properties including **the scaling laws of visual generation, the impact on original language capabilities, and the interrelation between visual understanding and generation tasks**.

We first revisit the plain design of MLLMs and present Liquid, a scalable decoder-only architecture for multi-modal generation and understanding. We employ the VQGAN [15] as image tokenizer to encode images into discrete tokens, similar to how a BPE processes text. This allows images and text to share the same vocabulary space, enabling LLMs to understand and generate images without any structural modifications. We find that existing LLMs are excellent starting points for training, as they have already acquired strong semantic understanding and generation capabilities. Compared to training from scratch like Chameleon [60], this approach saves $100\times$ of training cost while achieving stronger multimodal capabilities. We employ language data and image-text pair data to train six different sizes of LLMs, ranging from 0.5B to 32B across various model families. For each model, we create three distinct versions by training with text-only data, image generation data, and a combination of both tasks. This approach allows us to analyze the performance and interrelation between these tasks across different scales.

Our experiments reveal several insightful properties: 1) Directly employing LLMs for visual generation exhibits **clear scaling laws** in both validation loss and image consistency metrics, consistent with those seen in LLMs, regardless of whether the models retain their language capabilities or focus solely on visual generation tasks. 2) When trained with multimodal data such as image-text pairs and pure language data, the language capabilities of the models are lower compared to those trained with only language data. However, this **tradeoff diminishes as the model size increases**, indicating that larger models have sufficient capacity to handle both tasks seamlessly. This, combined with the scaling law, demonstrates the strong potential of LLMs as unified multimodal generator. 3) **The visual understanding and visual generation tasks can mutually benefit each other.** We find that increasing the data for either visual generation or visual understanding tasks improves the performance of the other, demonstrating the advantages and natural rationale of this paradigm in joint optimization.

We evaluate the capabilities of Liquid across text-guided image generation, visual understanding, and general text-only tasks. For image generation, Liquid outperforms other auto-regressive based models, as well as some diffusion models like SD-XL and achieve FID of 5.47 on MJHQ-30K, demonstrating that LLMs can acquire excellent imagery capabilities efficiently with a limited amount of data. For visual understanding, Liquid surpasses Chameleon and achieved results comparable to those of well-established MLLMs. In text-only tasks, Liquid achieves comparable performance with Chameleon, which used mix pre-training on a very large scale, and surpasses the performance of LLAMA2, demonstrating undegraded linguistic capabilities.

In summary, the main contributions of this paper can be categorized into the following points:

- An efficient decoder-only multi-modal generation framework that seamlessly carries out visual generation, visual comprehension, and pure language tasks.
- Comprehensive experiments about scaling laws of unified multi-modal models, revealing that the trade-off between language and visual tasks diminishes as scale of model increases.

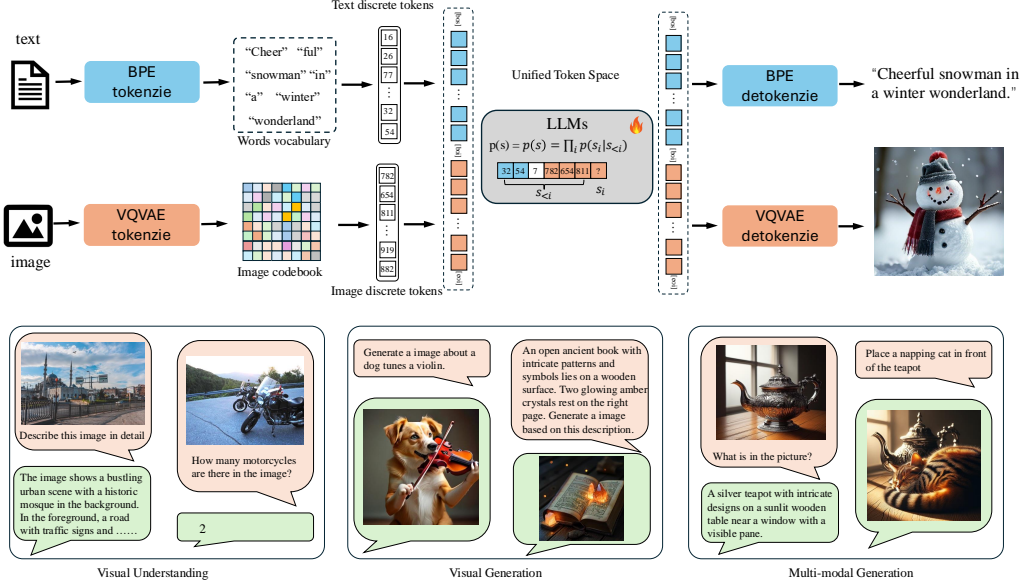


Figure 1: Pipeline of Liquid. The structure of Liquid follows a consistent format that treats images in the exact same way as text. A VQVAE based image tokenizer transforms the input images into discrete codes, which share the same vocabulary and embedding space with text codes. The image tokens and text tokens, once mixed, are fed into the LLMs and trained in the form of next token prediction. The lower part of the figure demonstrates that Liquid can handle various multi-modal understanding and generation tasks.

- An insightful discovery regarding the mutual boost of visual understanding and generation tasks within LLMs through the unification of visual tokens, highlighting the potential of LLMs to improve both understanding and generation capabilities by mixtraining.

2 Preliminaries

Image Tokenizer. We use the same tokenizer as Chameleon [60], which is a VQGAN [15]. It encodes a 512×512 image into 1024 discrete tokens in a codebook of size 8192. We appended these discrete image tokens to the text codebook produced by the BPE [54] tokenizer to expand the vocabulary size of the LLMs, thereby extending its language space to a multi-modal space encompassing both visual and linguistic elements.

Architecture. As illustrated in Fig. 1, Liquid can be constructed based on any existing LLMs. In this paper, we employ the GEMMA-7B [61] as base model of Liquid to validate its multimodal understanding, image generation capabilities, and performance on text-only tasks after augmenting it with the ability to understand and generate images. Then we conduct a comprehensive empirical study on the scaling behavior at scales of 0.5B, 1B, 2B, 7B, 9B, and 32B models from LLAMA-3 [14], GEMMA-2 [62], and Qwen2.5 [24]. We refrain from altering any structures within the LLMs to facilitate continued training directly from pre-trained weights. The only modification is the addition of 8192 new learnable embeddings for discrete image tokens. The LLMs maintain their original next-token prediction training objective with the standard cross-entropy loss.

Data Preparation. To maintain the language abilities of pre-trained LLMs, we sample text-only data from public datasets for the pre-training stage. We sample 15M text data from DCLM [28], 12M from SlimPajama [56], and 3M code data from Starcoderdata [31], totaling 30M text instances for approximately 60 billion text tokens. For image-text pairs, we use JourneyDB [44] and internal MidJourney-style synthetic data to compile 30M high-quality image data, for a total of 30 billion image tokens. All the data are used to form a hybrid multi-modal data for continue pre-training, resulting in quick acquisition of decent image generation capabilities while retaining language



Figure 2: The generated samples from Liquid-7B, showcase excellent capabilities in crafting high aesthetic and described-consistent images.

abilities. Furthermore, we reversed 20% of text-to-image data to train LLMs in a captioning task to enhance their visual understanding abilities.

Training Procedure. We use a total of 60M data to continue pretraining our models. For all image-text data, we define the input format for multi-modal training data as:

[bos] {text token} [boi] {image token} [eoi][eos] .

Here, [bos] and [eos] are the begin-of-sequence and end-of-sequence tokens defined in the original text tokenizer. We incorporate two additional spatial tokens, [boi] and [eoi] to signify the start and end of image tokens. In the scaling experiments, for each model size, we independently use 30M text-only data, 30M text-to-image data, and a mixed dataset of 60M data to train three different versions of the models. We then evaluate their performance on a series of tasks.

3 Experiments

3.1 How Well Do LLMs Perform in Visual Generation?

In this section, we comprehensively evaluate the visual generation capabilities of Liquid-7B model that have been continuously pretrained with a combined dataset of 60M mixed multimodal data. Subsequently, we evaluate mixed pre-trained models across six different sizes, ranging from 0.5B to 32B, the objective is to explore the scaling behavior of LLMs in visual generation tasks, while simultaneously preserving their linguistic capabilities.

Table 1: Comparison of VQAScore with other visual generation methods on GenAI-Bench. The basic prompts primarily focus on aspects such as scene, attribute, and relation, while the advanced prompts place a greater emphasis on counting, comparison, differentiation, and logic. The advanced prompts require complex visio-linguistic reasoning and present a significantly higher level of difficulty. Liquid outperforms all auto-regressive unified MLLMs on both types of prompts and has even surpassed some well-established diffusion models like SD v2.1 [51] and SD-XL [45]. It demonstrates that the images generated by Liquid align well with the input text prompts.

Method	Type	#Training Images	Attribute↑	Scene↑	Relation↑			Overall↑
					Spatial	Action	Part	
SD v2.1 [51]	Diffusion	2000M	0.80	0.79	0.76	0.77	0.80	0.78
SD-XL [45]	Diffusion	2000M	0.84	0.84	0.82	0.83	0.89	0.83
Midjourney v6 [47]	Diffusion	–	0.88	0.87	0.87	0.87	0.91	0.87
DALL-E 3 [35]	Diffusion	–	0.91	0.90	0.92	0.89	0.91	0.90
Show-o [71]	Discrete Diff.	36M	0.72	0.72	0.70	0.70	0.75	0.70
LWM [40]	Autoregressive	–	0.63	0.62	0.65	0.63	0.70	0.63
VILA-U [70] (256)	Autoregressive	15M	0.78	0.78	0.77	0.78	0.79	0.76
VILA-U [70] (384)	Autoregressive	15M	0.75	0.76	0.75	0.73	0.75	0.73
Liquid-7B	Autoregressive	30M	0.84	0.86	0.81	0.83	0.91	0.83

(a) VQAScores on <i>basic</i> prompts of GenAI-Bench								
Method	Type	#Training Images	Count↑	Differ↑	Compare↑	Logical↑		Overall↑
						Negate	Universal	
SD v2.1 [51]	Diffusion	2000M	0.68	0.70	0.68	0.54	0.64	0.62
SD-XL [45]	Diffusion	2000M	0.71	0.73	0.69	0.50	0.66	0.63
Midjourney v6 [47]	Diffusion	–	0.78	0.78	0.79	0.50	0.76	0.69
DALL-E 3 [35]	Diffusion	–	0.82	0.78	0.82	0.48	0.80	0.70
Show-o [71]	Discrete Diff.	36M	0.70	0.62	0.71	0.51	0.65	0.60
LWM [40]	Autoregressive	–	0.59	0.58	0.54	0.49	0.52	0.53
VILA-U [70] (256)	Autoregressive	15M	0.70	0.71	0.74	0.53	0.66	0.64
VILA-U [70] (384)	Autoregressive	15M	0.68	0.67	0.71	0.51	0.64	0.61
Liquid-7B	Autoregressive	30M	0.76	0.73	0.74	0.46	0.74	0.65

(b) VQAScores on <i>advanced</i> prompts of GenAI-Bench								
Method	Type	#Training Images	Count↑	Differ↑	Compare↑	Logical↑		Overall↑
						Negate	Universal	
SD v2.1 [51]	Diffusion	2000M	0.68	0.70	0.68	0.54	0.64	0.62
SD-XL [45]	Diffusion	2000M	0.71	0.73	0.69	0.50	0.66	0.63
Midjourney v6 [47]	Diffusion	–	0.78	0.78	0.79	0.50	0.76	0.69
DALL-E 3 [35]	Diffusion	–	0.82	0.78	0.82	0.48	0.80	0.70
Show-o [71]	Discrete Diff.	36M	0.70	0.62	0.71	0.51	0.65	0.60
LWM [40]	Autoregressive	–	0.59	0.58	0.54	0.49	0.52	0.53
VILA-U [70] (256)	Autoregressive	15M	0.70	0.71	0.74	0.53	0.66	0.64
VILA-U [70] (384)	Autoregressive	15M	0.68	0.67	0.71	0.51	0.64	0.61
Liquid-7B	Autoregressive	30M	0.76	0.73	0.74	0.46	0.74	0.65

(b) VQAScores on *advanced* prompts of GenAI-Bench

3.1.1 Quantitative Results on Visual Generation Benchmarks

For the image generation tasks, we evaluate the model on two benchmarks, GenAI-Bench [36] and MJHQ-30K [27]. GenAI-Bench is a challenging image-to-text generation benchmark designed to evaluate the capabilities of visual generation models. It evaluates both basic skills, such as understanding attributes, scenes, and relations in text inputs, and advanced skills, including abilities like counting, differentiation, comparison, and understanding logical relationships from text input, thereby highlighting the graded progression in complexity. GenAI-Bench employs VQAScore, which leverages a visual-question-answering (VQA) model. This enables more precise evaluation of how well the generated image aligns with the text prompt, critically assessing the capability to parse scenes, objects, attributes, relationships, and engage in higher-order reasoning such as comparison and logic. The latter calculates the Frechet Inception Distance (FID) [22] score between the generated images and 30K high-quality images to assess the quality of the generated images.

As shown in Tab. 1, compare with other auto-regressive based methods, Liquid achieves a better overall score under both basic prompts and advanced prompts. This suggests that the images generated by Liquid align better semantically with the input text prompts. Notably, Liquid also outperforms

Table 2: Comparison with other visual generation methods on MJHQ-30K evaluation benchmark. The FID of Liquid is lower than that of all the auto-regressive models and even outperforms most diffusion models. This indicates that the images generated by Liquid have superior aesthetic quality.

Method	Type	#Images	FID↓
SD-XL [45]	Diffusion	2000M	9.55
PixArt [6]	Diffusion	25M	6.14
Playground v2.5 [27]	Diffusion	–	4.48
Show-o [71]	Discrete Diff.	36M	15.18
LWM [40]	Autoregressive	–	17.77
VILA-U (256) [70]	Autoregressive	15M	12.81
VILA-U (384) [70]	Autoregressive	15M	7.69
Janus [69]	Autoregressive	–	10.10
Liquid-7B	Autoregressive	30M	5.47

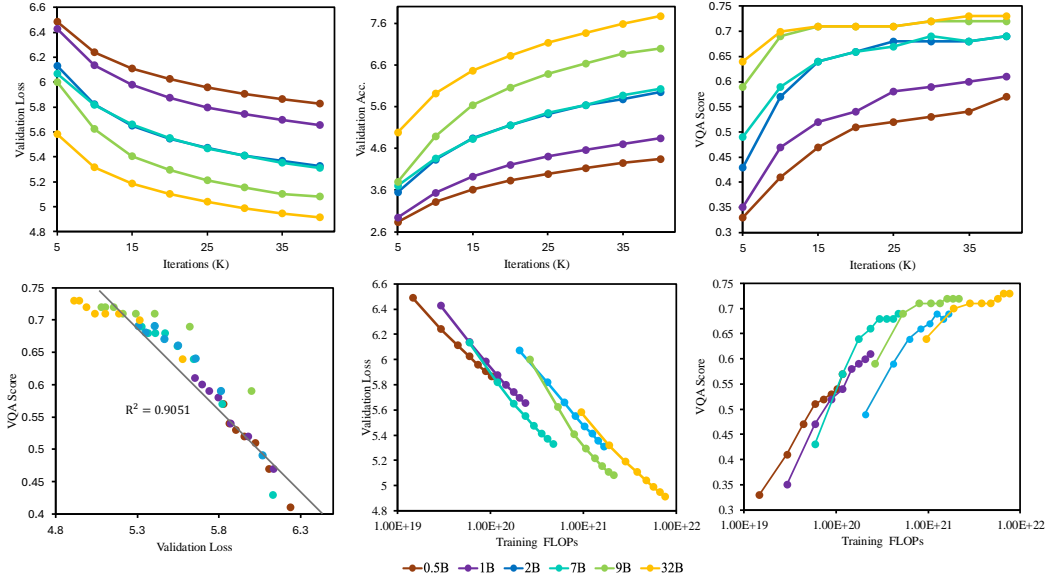


Figure 3: **Scaling behavior of LLMs in multimodal generation across different sizes.** We explore the visual generation performance of LLMs ranging from 0.5B to 32B in size after undergoing mixed training with language data and text-to-image data. The validation loss smoothly decreases as both the model size and training iterations increase, while token accuracy and VQA Score consistently rise. The VQA Score consistently increases as the validation loss decreases, indicating a strong correlation between them. Under the same training FLOPs, smaller models reach lower validation losses more quickly, but larger models ultimately achieve higher evaluation metrics.

some well-established diffusion models like SD v2.1 [51] and SD-XL[45] for both basic and advanced prompts. Compared to these diffusion models, Liquid utilizes significantly fewer image data, which indicating that learning based on LLMs can assist the model in understanding the semantic association between the generated content and prompts, while also offering higher training efficiency. Moreover, it demonstrates that LLMs have strong potential for generating complex visual content.

In Tab. 2, we report FID on MJHQ-30K to compare the images quality generated by Liquid with other models. It is observable that Liquid not only has a lower FID than all other auto-regressive methods but also surpasses most well-known diffusion models except Playground v2.5 [27], achieving a very low FID of 5.47. It indicates that LLMs are also capable of generating high-quality images, as shown in Fig. 2, providing proof that the upper limit of LLMs in terms of image aesthetic quality is not inferior to diffusion models. Further more, due to the capability of LLM to generate dynamically-length content in the form of next-token prediction, the convenience can be applied to visual generation. We find that by appending instructions about the resolution to the input text prompt, such as "length is: width is:", the model can quickly learn to generate the corresponding code according to the specified number of rows and columns. Fig. 2 demonstrates the generation results at various resolutions, showcasing the flexibility of Liquid.

3.1.2 Scaling Results on Visual Generation

We explore the visual generation performance of LLMs ranging from 0.5B to 32B in size after mixed training with language data and text-to-image data. As shown in Fig. 3, with the increase in model size and training iterations, the validation loss smoothly decreases, while token accuracy and VQA Score consistently increase. Moreover, the VQA score continues to rise as the validation loss decreases, indicating a strong correlation between validation loss and holistic image evaluation metrics. Under the same training FLOPs, smaller models achieve lower validation losses and higher VQA Scores more quickly, but larger models ultimately reach higher evaluation metrics. This may be due to smaller models being able to iterate through more training steps rapidly, allowing for swift changes in model capabilities. Although smaller models can quickly acquire visual generation abilities, their upper limits are lower, making it difficult to achieve high-quality visual generation results. As shown in Fig. 4, larger models eventually obtain more robust visual generation outcomes.

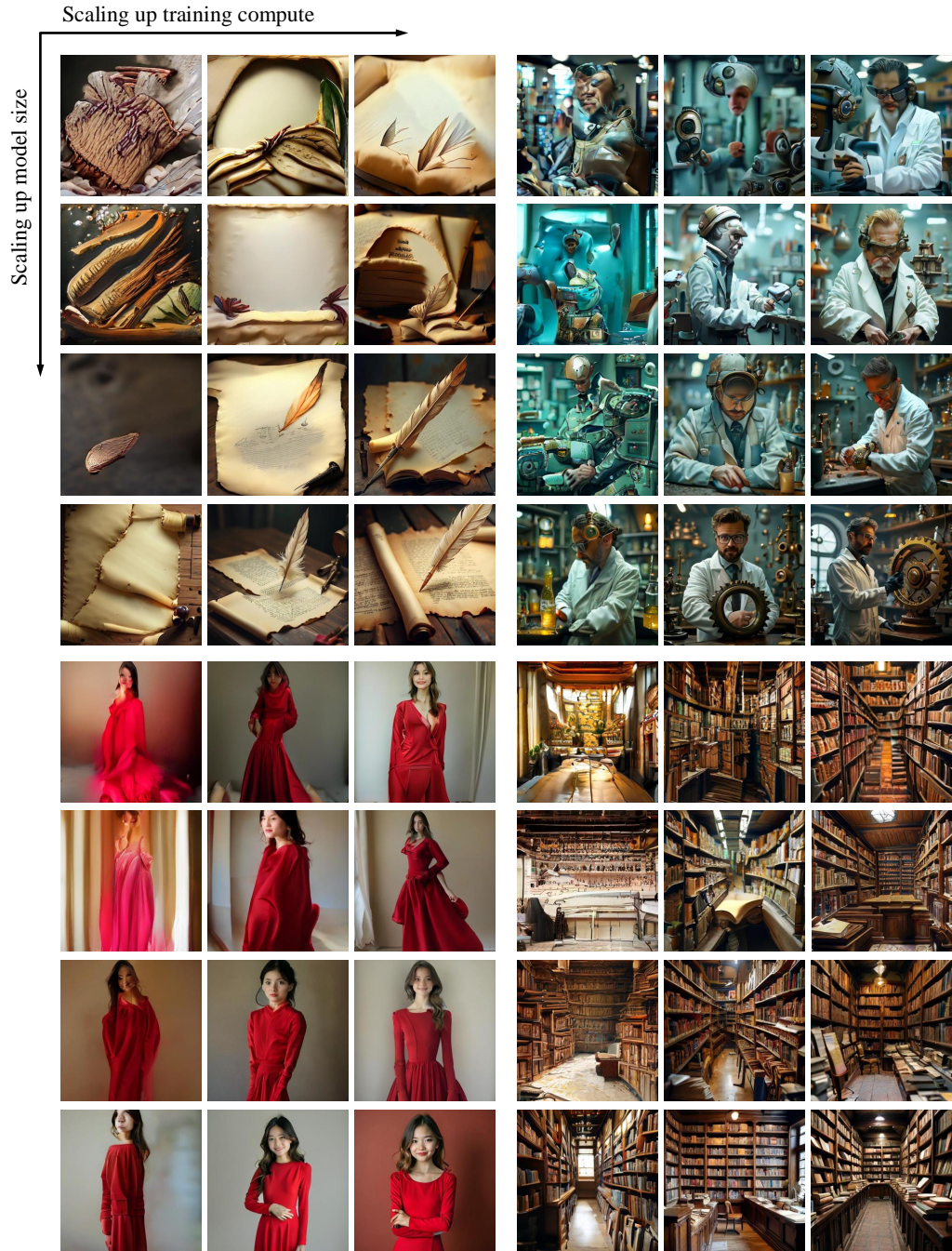


Figure 4: Scaling model size and training compute improves visual fidelity and soundness. Zoom in for a better view. Samples are drawn from Liquid models of 4 different sizes (0.5B, 1B, 2B, 9B) and 3 different training steps (5K, 15K, 40K).

3.2 Does Visual Generation Compromise Language Ability?

In this section, we evaluate the impact on the inherent linguistic capabilities of LLMs after they acquire visual generation abilities. First, we compare the continuously pretrained GEMMA-7B base model with mainstream language models to determine if it has retained robust linguistic capabilities. Subsequently, we evaluate LLMs of different sizes that have been trained either exclusively with 30M language data or with a mix of 60M multimodal data. Since both training processes use the same

language data, this allows for a fair comparison of how different sizes of LLMs are affected in terms of their original linguistic capabilities after acquiring visual generation abilities.

3.2.1 Comparison with Mainstream LLMs

To validate whether acquiring image understanding and generation capabilities has any impact on the original language abilities of the LLMs, we report overall zero-shot performance across a suite of popular benchmarks that measure commonsense reasoning and reading comprehension capabilities: HellaSwag [74], WinoGrande [52], ARC-Easy [10], ARC-Challenge [10], OpenBookQA [43], PIQA [3], SIQA [53], and BoolQ [9]. We also perform an evaluation of the 5-shot results on MMLU [21], a comprehensive benchmark that measures world/in-domain knowledge and problem-solving skills across 57 subjects.

We evaluate the general text-only capabilities of our mixed multimodal pretrained model against other state-of-the-art large language models and multi-modal language models, following the evaluation protocol of [17]. As shown in Tab. 3, Liquid outperforms the well-established language model LLAMA2 [65] and the mix-pretrained multi-modal language model Chameleon [60] in most tasks, exhibiting undegraded linguistic capabilities. Compared with Chameleon [60], which is mixed pretrained with an extremely large scale of data, Liquid performs training from existing LLMs that already possess decent language capabilities, maintaining these capabilities without degradation. This result validates the efficiency of our training framework and demonstrates that with this framework, we can extend the visual generation and understanding capabilities to LLMs of any structure and size.

Table 3: Performance of pre-trained model on standard text-only benchmarks. Liquid outperforms the well-established language model LLAMA2 and the mix-pretrained multi-modal language model Chameleon in most tasks, exhibiting undegraded linguistic capabilities.

Method	BoolQ	PIQA	SIQA	HellaSwag	WinoGrande	ARC-e	ARC-c	MMLU
Mistral	7B	84.7	83.0	-	81.3	75.3	80.0	55.5
	8×7B	-	83.6	-	84.4	77.2	83.1	59.7
LLAMA2	7B	77.4	78.8	48.3	77.2	69.2	75.2	45.9
	13B	81.7	80.5	50.3	80.7	72.8	77.3	49.4
	34B	83.7	81.9	50.9	83.3	76.7	79.4	54.8
Chameleon	7B	81.4	79.6	57.0	74.2	70.4	76.1	46.5
	34B	86.0	83.3	63.3	82.7	78.5	84.1	59.7
Liquid-7B	7B	81.0	81.0	46.7	76.1	72.7	75.6	49.0
								56.0

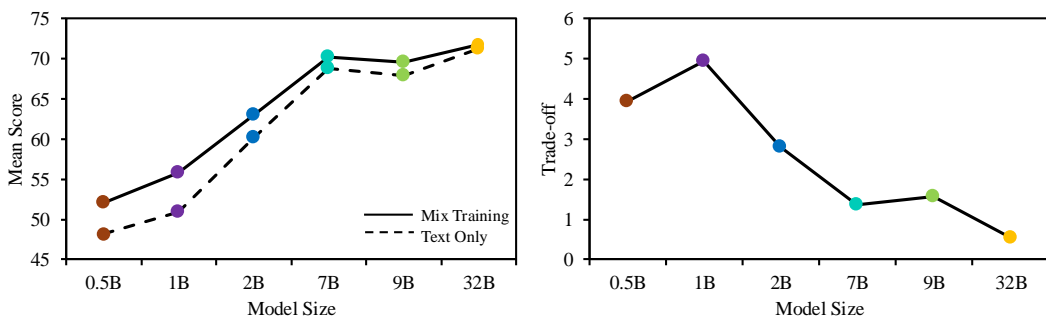


Figure 5: The performance impact of multi-modal mixed training versus text-only training on language tasks. Multi-modal mixed training does impact language performance when the model size is small. However, this degradation gradually disappears as the model size increases.

3.2.2 Scaling Results on Language Tasks

To investigate whether visual generation capabilities impact linguistic abilities, we compare the performance of models trained with 30M language data and those trained with a mix of 60M

multimodal data on language tasks across different sizes. For language ability, we report the average average scores on 5 language tasks, including HellaSwag, WinoGrande, ARC-Easy, ARC-Challenge, and BoolQ. As shown in Fig. 5, we find a trade-off phenomenon when both tasks were mixed in the training of smaller models; however, as the model size increased, this trade-off gradually disappeared. This confirms that larger models possess sufficient capacity to handle both visual and language spaces generation concurrently.

3.3 Does Language Ability Limit Visual Generation Performance?

In language tasks, we observe a trade-off in performance of multimodal LLMs, raising the question of whether this trade-off also exists in visual generation tasks. To address this question, we compare LLMs of different sizes that have been trained exclusively with text-to-image data and with a mix of multimodal data. Both training utilize the same visual generation data, with the only difference being whether the models retain their linguistic capabilities.

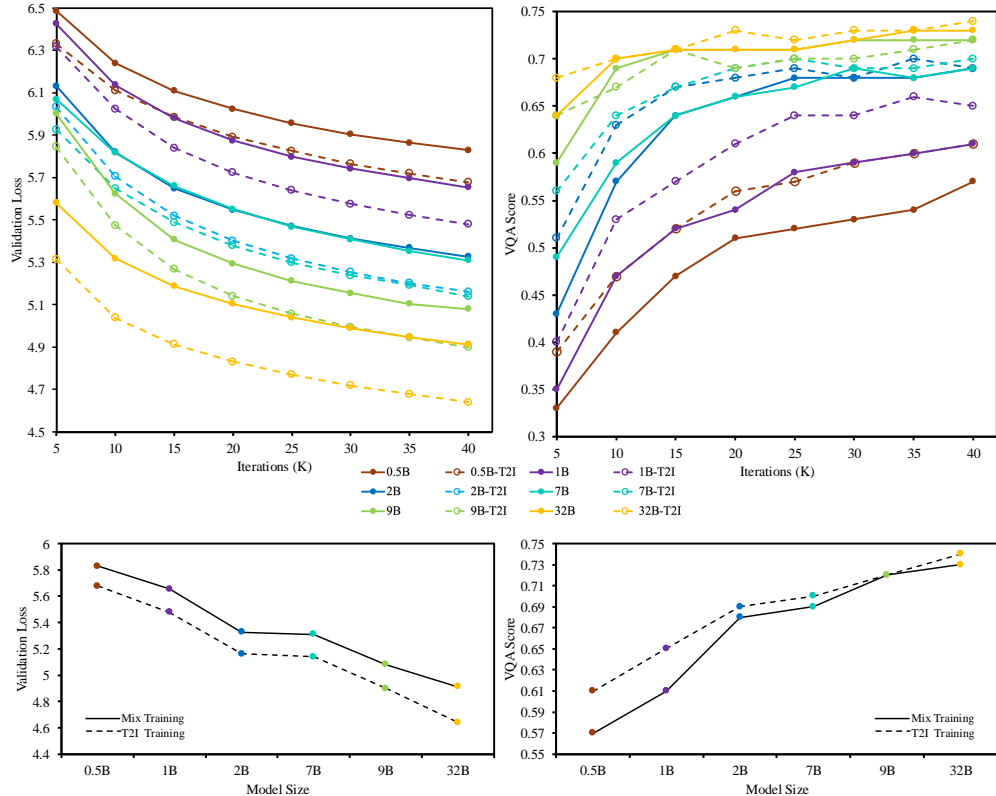


Figure 6: Scaling results between T2I only training and Mix training. Mix training results in higher validation loss on visual generation tasks for models of every size. However, its impact on the VQA Score diminishes as the size of the model increases.

As illustrated in Fig. 6, mixed training leads to higher validation loss on visual generation tasks for models of every size. However, the detrimental effect on the VQA Score decreases as the model size increases. This reduction is partly due to the increased capacity of larger models and may also be attributed to the evaluation metrics approaching saturation. Nevertheless, it can be argued that as the size of the model increases, the trade-off between visual generation and language tasks gradually diminishes or even disappears. This encourages leveraging the scaling capabilities of LLMs into multimodal models.

3.4 How Does Liquid Perform on Visual Understanding Tasks?

After the pre-training stage, the model has already attained substantial image generation capabilities and a decent level of image understanding. To evaluate the visual understanding capabilities, we use

Table 4: Comparison with leading methods on visual language benchmarks. * indicates that images in the training split of these datasets are observed during training. “Und.” and “Gen.” denote “understanding” and “generation”. Our performance surpasses most models that unify understanding and generation, and it is comparable with models dedicated to visual understanding in some tasks. † has a longer pre-training phase, can further enhance its performance.

Type	Method	LLM	Visual Token	Res.	VQAv2	GQA	TextVQA	POPE	MME
Und. Only	LLaVA-1.5 [39]	Vicuna-1.5-7B	Continuous	336	78.5*	62.0*	58.2	85.9	1510.7
	VILA [34]	LLaMA-2-7B	Continuous	336	79.9*	62.3*	64.4	85.5	1533.0
	InstructBLIP [11]	Vicuna-7B	Continuous	224	—	49.2	50.1	—	—
	IDEFICS-9B [26]	LLaMA-7B	Continuous	224	50.9	38.4	25.9	—	—
Und. & Gen.	Unified-IO 2 [41]	6.8B from scratch	Continuous	384	79.4*	—	—	87.7	—
	Emu [59]	LLaMA-13B	Continuous	224	52.0	—	—	—	—
	LaVIT [25]	LLaMA-7B	Continuous	224	66.0	46.8	—	—	—
	DreamLLM [13]	Vicuna-7B	Continuous	224	72.9*	—	41.8	—	—
	CM3Leon-7B [73]	7B from scratch	Discrete	256	47.6	—	—	—	—
	LWM [40]	LLaMA-2-7B	Discrete	256	55.8	44.8	18.8	75.2	—
	Show-o [71]	Phi-1.5-1.3B	Discrete	256	59.3*	48.7*	—	73.8	948.4
	VILA-U [40]	LLaMA-2-7B	Discrete	256	75.3*	58.3*	48.3	83.9	1336.2
	Chameleon [60]	34B from scratch	Discrete	512	69.6	—	—	—	—
	Ours	Gemma-7B	Discrete	512	68.0*	56.1*	40.4	81.1	1107.2
	Ours†	Gemma-7B	Discrete	512	71.3*	58.4*	42.4	81.1	1119.3

1M LMSYS [75] as text-only instruction data, coupled with 1M text-to-Image data sampled from high-quality data, and 1.5M multi-modal instruction tuning data introduced in Minigemini [33]. This compiles a 3.5M hybrid instruction tuning data for further refining our model. We report results on widely-adopted zero-shot image-based benchmarks, which include VQA-v2 [20], GQA [23], TextVQA [55], POPE [32], and MME [16].

As shown in Tab. 4, compare with the MLLMs with discrete visual token, Liquid outperforms models with stander VQVAE like LWM [40], Chameleon [60], and Show-o [71], and achieves comparable results with VILA-U [70], which have trained a CLIP based multi-codebook VQVAE to improve understanding. However, the performance of MLLMs using discrete visual tokens on visual understanding tasks tends to be lower than mainstream models that employ continuous visual tokens. Most MLLMs with continuous visual token use CLIP features as visual input, it is a significant advantage considering that CLIP is pre-trained on a large-scale image-text pair dataset, leading to a strong alignment between its visual space features and language space features. This alignment substantially aids the LLMs, making it easier for them to understand visual content. In contrast, using image tokens derived directly from VQVAE tokenizer as input means that the corresponding embedding features in the LLM are reinitialized with out any alignment. Without extensive pre-training to align feature spaces, the visual understanding capabilities might be slightly inferior to models using CLIP as visual input. The difference in performance mainly stems from the fact that most VQVAE currently do not align image-text spaces. VILA-U [70] has confirmed that by adding CLIP loss during the VQVAE training to align its visual space, the performance of visual understanding tasks can be improved.

However, we attempt to increase the amount of image-text pairs the model can see during the pre-training phase by training one more epoch on our multi-modal pre-training data, and then we were surprised to discover that the model could achieve better performance on visual understanding tasks. This result indicates that mixed-modality pre-training plays a role similar to CLIP pre-training, aligning text and visual embedding spaces. More pret-raining or more suitable embedding initialization methods could further boost the performance of discrete visual tokens on visual understanding tasks.

3.5 Will Understanding and Generation Tasks Mutually Improve Each Other?

As observed in above experiments on visual understanding tasks, extended pretraining enhances comprehension abilities. Notably, during the pretraining process, 80% of the data was trained in a text-to-image format. This observation naturally leads us to question whether increased training with text-to-image data could improve performance on understanding tasks. Furthermore, we explore whether there is a synergistic relationship between these two tasks.

We conduct three sets of experiments. In the first set, we used a combination of 10M text-only data, 10M visual generation data, and 10M visual understanding data, resulting in a total of 30M data for the pre-training phase. The visual understanding data is derived by reversing the visual generation data for the captioning task, and the loss is calculated only on the text output for visual understanding task. All data are subsets of the data introduced in Section 3. The experiment, with a 1 : 1 : 1 data ratio of the three tasks, serves as the baseline. Building on this baseline, we separately add an additional 10M visual generation data and 10M visual understanding data, forming a total of 40M data with data ratios of 1 : 2 : 1 and 1 : 1 : 2, respectively, labeled as ‘Add T2I’ and ‘Add I2T’. We train three GEMMA-7B models using default parameters and evaluate their performance on visual understanding and generation tasks to observe the impact of different data additions on the performance of all tasks. For the visual understanding tasks, after the pre-training phase, we perform the same instruction tuning training and then test them on standard visual understanding benchmarks.

Table 5: The impact between visual understanding and generation tasks. “Visual Gen.” refers to the data used for training text-guided image generation, while “Visual Und.” refers to the data used for training visual understanding capabilities, specifically in the form of captioning. Compared to the baseline, adding more visual understanding data enhances the visual generation capability, improving the semantic consistency between the generated content and the prompt. Conversely, increasing the visual generation data similarly aids in enhancing the model’s visual understanding ability. This indicates that when the tokens for visual generation and understanding are unified, they share a common optimization objective and can mutually enhance each other.

Method	Training Data			Visual Generation			Visual Understanding				
	Text-only	Visual Gen.	Visual Und.	Basic	Advanced	Overall	VQAv2	GQA	TextVQA	POPE	MME
Baseline	10M	10M	10M	0.63	0.58	0.60	60.7	51.3	39.2	75.9	909.6
Add T2I	10M	20M	10M	0.78	0.63	0.69	64.5	53.2	39.8	78.0	1066.8
Add I2T	10M	10M	20M	0.73	0.62	0.66	63.5	53.7	40.5	76.8	1035.1

As shown in Tab. 5, we observe that adding more visual understanding data during pre-training significantly improves the performance of visual generation tasks. Conversely, adding more visual generation data further enhances the performance of visual understanding tasks. This important phenomenon indicates that when the modality spaces for visual understanding and generation are unified, the training of these two tasks can mutually benefit each other. Intuitively, when images are represented using embeddings from the same space, both visual generation and visual understanding tasks require stronger consistency constraints and sufficient interaction between language and visual information. Therefore, the optimization directions for these two tasks are very similar. This further demonstrates the potential of LLMs as general-purpose multi-modal generators. The continuous addition of visual training data can simultaneously enhance the models’ capabilities in both multimodal understanding and generation.

4 Related Work

Multi-modal Large Language Models. The rapid advancement of Large Language Models (LLMs) [8, 4, 64, 65, 61] in recent years has inspired researchers to explore their application in visual understanding tasks. The integration of visual information with language models brings about potent multi-modal comprehension and reasoning abilities. Initial works such as LLaVA [39] and MiniGPT4 [77] propose to project features from a pre-trained visual foundation model [46, 30] into the feature space of LLMs, exhibiting encouraging multi-modal understanding capacities. Building upon this progress, an array of MLLMs [1, 29, 11, 2] have been well-designed and extensively trained on comprehensive vision-language data, achieving noteworthy performance on visual understanding and reasoning tasks. The LLaVA series [39, 37, 42, 5, 7, 38, 33] employ image-text pair data to train a projector, projecting the image-feature from CLIP to align the language spaces within the input space of LLMs. They further enhance visual understanding and reasoning abilities by training the entire pipeline via a curated multi-modal instruction tuning dataset. Despite their robust multi-modal understanding capabilities, existing models are primarily focused on visual understanding, falling short on generating visual outputs that extend beyond text.

Vision Generation. In the past few years, the realm of visual generation has been primarily dominated by diffusion models [45, 51, 47, 35, 49], which progressively generate high-quality, high-resolution images via a diffusion process over a continuous latent space. Several efforts [18, 19, 25, 59, 58, 68]

have attempted to extend LLMs with pretrained diffusion models to integrate image generation capabilities. These studies employ diffusion models as a tool where the diffusion models generate images conditioned on the features output by the LLMs. In this combination, LLMs merely contribute the semantic feature output and lack the direct ability to generate visual content. Moreover, the upper limit of visual generation capacity is dictated by the pre-trained diffusion model, leaving the inherent potential of LLMs in visual generation under-explored.

An alternative viable approach involves using autoregressive models to generate images by predicting the next token in a sequence, as exemplified by models like DALL-E [50], CogView [12], Parti [72] and LlamaGen [57]. Visual AutoRegressive modeling (VAR)[63] redefined auto-regressive learning on images as coarse-to-fine “next-scale prediction”. It demonstrates superior generalization and scaling capabilities compared to diffusion transformers while requiring fewer steps. These models typically employ VQVAE [15] to tokenize images into a set of discrete codes, subsequently training a decoder-only transformer to predict image codes which are then detokenized back to images. These approaches showcase the potential of decoder-only LLMs in directly conducting image generation. However, they often fail to match the performance of diffusion models and do not explore the possibility of unified output between visual and linguistic modalities. In this work, our objective is to enable LLMs to generate visual content via next-token prediction without altering their structure or capabilities, and explore the characteristics that emerge from the combination of these two tasks within LLMs.

Unified Multimodal Understanding and Generation Several early efforts have explored how to construct a unified multi-modal large model for visual generation and understanding based on LLMs. The central challenge lies in tokenizing images into sequence inputs for the LLMs and detokenizing the sequential output of the LLMs back into images, the choice of image tokenizer. Some methods [18, 19, 59, 58] use vision encoders based on ViT like CLIP to encode images into continuous feature maps. The continuous visual space from CLIP can retain more visual information and have a pre-trained, aligned space with language feature. However, the continuous feature often necessitates an additional diffusion module for image detokenization. Other works [40, 60, 70] employ VQVAE to encode images into discrete tokens and train LLMs to predict them. Still other works [41, 71, 69] use both ViT and VQVAE as tokenizers to garner their benefits. Discrete image features can share the same embedding space with text input, permitting joint reasoning over both modalities within a unified architecture without the requirement for modality-specific components. It is beneficial for model scale-up. Consequently, in our work, we choose VQVAE as the sole image tokenizer. Our work is most similar to LWM [40] and Chameleon [60]. However, they display inferior image understanding and generation capabilities, and need extensive large scale multi-modal pre-training, which is a significant burden. In contrast, we propose to start from any existing LLMs and enhance their visual understanding and generation abilities by continuing training with a small amount of high-quality data, without altering any model structures.

5 Conclusion

In this paper, we present Liquid, an efficient framework enabling language models to acquire image generation and understanding capabilities without modifying the original structure. Unlike traditional multi-modal models employing extra visual models, Liquid directly tokenize images into discrete tokens that share the same embedding space with text tokens. This leads to a total unification of images and text within the models, which stokes the potential of multi-modal learning. Utilizing various existing LLMs provides a unique advantage to Liquid, enabling it to scale up easily and display similar scaling behavior to LLMs.

Leveraging this convenience, we conducted extensive scaling experiments on models ranging from 0.5B to 32B across different model families. We identified some key characteristics of multimodal models under this unified token space. 1) Firstly, by directly training LLMs on visual generation tasks, they can retain foundational language capabilities while achieving results comparable to some mainstream diffusion models. 2) Secondly, this unification of multimodal tasks tends to impair both visual generation and language tasks; however, this impairment gradually diminishes as the model size increases. 3) Lastly, we found that when visual and language tokens are represented uniformly, visual understanding and generation tasks can mutually enhance each other. This reciprocity encourages the vast potential of large-scale pretraining under this paradigm.

References

- [1] J.-B. Alayrac, J. Donahue, P. Luc, A. Miech, I. Barr, Y. Hasson, K. Lenc, A. Mensch, K. Millican, M. Reynolds, et al. Flamingo: a visual language model for few-shot learning. *Advances in Neural Information Processing Systems*, 35:23716–23736, 2022. 11
- [2] J. Bai, S. Bai, S. Yang, S. Wang, S. Tan, P. Wang, J. Lin, C. Zhou, and J. Zhou. Qwen-vl: A frontier large vision-language model with versatile abilities. *arXiv preprint arXiv:2308.12966*, 2023. 11
- [3] Y. Bisk, R. Zellers, J. Gao, Y. Choi, et al. Piqa: Reasoning about physical commonsense in natural language. In *Proceedings of the AAAI conference on artificial intelligence*, pages 7432–7439, 2020. 8
- [4] T. Brown, B. Mann, N. Ryder, M. Subbiah, J. D. Kaplan, P. Dhariwal, A. Neelakantan, P. Shyam, G. Sastry, A. Askell, et al. Language models are few-shot learners. *Advances in neural information processing systems*, 33:1877–1901, 2020. 1, 11
- [5] G. H. Chen, S. Chen, R. Zhang, J. Chen, X. Wu, Z. Zhang, Z. Chen, J. Li, X. Wan, and B. Wang. Allava: Harnessing gpt4v-synthesized data for a lite vision-language model. *arXiv preprint arXiv:2402.11684*, 2024. 1, 11
- [6] J. Chen, J. Yu, C. Ge, L. Yao, E. Xie, Y. Wu, Z. Wang, J. Kwok, P. Luo, H. Lu, et al. Pixart-alpha: Fast training of diffusion transformer for photorealistic text-to-image synthesis. *arXiv preprint arXiv:2310.00426*, 2023. 5
- [7] L. Chen, J. Li, X. Dong, P. Zhang, C. He, J. Wang, F. Zhao, and D. Lin. Sharegpt4v: Improving large multi-modal models with better captions. *arXiv preprint arXiv:2311.12793*, 2023. 11
- [8] A. Chowdhery, S. Narang, J. Devlin, M. Bosma, G. Mishra, A. Roberts, P. Barham, H. W. Chung, C. Sutton, S. Gehrmann, et al. Palm: Scaling language modeling with pathways. *arXiv preprint arXiv:2204.02311*, 2022. 1, 11
- [9] C. Clark, K. Lee, M.-W. Chang, T. Kwiatkowski, M. Collins, and K. Toutanova. Boolq: Exploring the surprising difficulty of natural yes/no questions. *arXiv preprint arXiv:1905.10044*, 2019. 8
- [10] P. Clark, I. Cowhey, O. Etzioni, T. Khot, A. Sabharwal, C. Schoenick, and O. Tafjord. Think you have solved question answering? try arc, the ai2 reasoning challenge. *arXiv preprint arXiv:1803.05457*, 2018. 8
- [11] W. Dai, J. Li, D. Li, A. M. H. Tiong, J. Zhao, W. Wang, B. Li, P. Fung, and S. Hoi. Instructblip: Towards general-purpose vision-language models with instruction tuning. *arXiv*, 2023. 10, 11
- [12] M. Ding, Z. Yang, W. Hong, W. Zheng, C. Zhou, D. Yin, J. Lin, X. Zou, Z. Shao, H. Yang, et al. Cogview: Mastering text-to-image generation via transformers. *Advances in neural information processing systems*, 34:19822–19835, 2021. 2, 12
- [13] R. Dong, C. Han, Y. Peng, Z. Qi, Z. Ge, J. Yang, L. Zhao, J. Sun, H. Zhou, H. Wei, et al. Dreamllm: Synergistic multimodal comprehension and creation. *arXiv preprint arXiv:2309.11499*, 2023. 10
- [14] A. Dubey, A. Jauhri, A. Pandey, A. Kadian, A. Al-Dahle, A. Letman, A. Mathur, A. Schelten, A. Yang, A. Fan, et al. The llama 3 herd of models. *arXiv preprint arXiv:2407.21783*, 2024. 3
- [15] P. Esser, R. Rombach, and B. Ommer. Taming transformers for high-resolution image synthesis. In *Proceedings of the IEEE/CVF conference on computer vision and pattern recognition*, pages 12873–12883, 2021. 2, 3, 12
- [16] C. Fu, P. Chen, Y. Shen, Y. Qin, M. Zhang, X. Lin, J. Yang, X. Zheng, K. Li, X. Sun, Y. Wu, and R. Ji. Mme: A comprehensive evaluation benchmark for multimodal large language models, 2024. 10
- [17] L. Gao, J. Tow, B. Abbasi, S. Biderman, S. Black, A. DiPofi, C. Foster, L. Golding, J. Hsu, A. Le Noac'h, H. Li, K. McDonell, N. Muennighoff, C. Ociepa, J. Phang, L. Reynolds, H. Schoelkopf, A. Skowron, L. Sutawika, E. Tang, A. Thite, B. Wang, K. Wang, and A. Zou. A framework for few-shot language model evaluation, 07 2024. 8
- [18] Y. Ge, Y. Ge, Z. Zeng, X. Wang, and Y. Shan. Planting a seed of vision in large language model. *arXiv preprint arXiv:2307.08041*, 2023. 1, 11, 12
- [19] Y. Ge, S. Zhao, J. Zhu, Y. Ge, K. Yi, L. Song, C. Li, X. Ding, and Y. Shan. Seed-x: Multimodal models with unified multi-granularity comprehension and generation. *arXiv preprint arXiv:2404.14396*, 2024. 1, 11, 12
- [20] Y. Goyal, T. Khot, D. Summers-Stay, D. Batra, and D. Parikh. Making the V in VQA matter: Elevating the role of image understanding in Visual Question Answering. In *Conference on Computer Vision and Pattern Recognition (CVPR)*, 2017. 10
- [21] D. Hendrycks, C. Burns, S. Basart, A. Zou, M. Mazeika, D. X. Song, and J. Steinhardt. Measuring massive multitask language understanding. *arXiv preprint arXiv:2009.03300*, 2020. 8
- [22] M. Heusel, H. Ramsauer, T. Unterthiner, B. Nessler, and S. Hochreiter. Gans trained by a two time-scale update rule converge to a local nash equilibrium. *Advances in neural information processing systems*, 30, 2017. 5
- [23] D. A. Hudson and C. D. Manning. Gqa: A new dataset for real-world visual reasoning and compositional question answering. In *Proceedings of the IEEE/CVF conference on computer vision and pattern recognition*, pages 6700–6709, 2019. 10
- [24] B. Hui, J. Yang, Z. Cui, J. Yang, D. Liu, L. Zhang, T. Liu, J. Zhang, B. Yu, K. Lu, et al. Qwen2. 5-coder technical report. *arXiv preprint arXiv:2409.12186*, 2024. 3

- [25] Y. Jin, K. Xu, L. Chen, C. Liao, J. Tan, B. Chen, C. Lei, A. Liu, C. Song, X. Lei, et al. Unified language-vision pretraining with dynamic discrete visual tokenization. *arXiv preprint arXiv:2309.04669*, 2023. 1, 10, 11
- [26] H. Laurençon, D. van Strien, S. Bekman, L. Tronchon, L. Saulnier, T. Wang, S. Karamcheti, A. Singh, G. Pistilli, Y. Jernite, et al. Introducing idefics: An open reproduction of state-of-the-art visual language model, 2023. URL <https://huggingface.co/blog/idefics>. Accessed, pages 09–18, 2023. 10
- [27] D. Li, A. Kamko, E. Akhgari, A. Sabet, L. Xu, and S. Doshi. Playground v2. 5: Three insights towards enhancing aesthetic quality in text-to-image generation. *arXiv preprint arXiv:2402.17245*, 2024. 5, 6
- [28] J. Li, A. Fang, G. Smyrnis, M. Ivgi, M. Jordan, S. Gadre, H. Bansal, E. Guha, S. Keh, K. Arora, S. Garg, R. Xin, N. Muennighoff, R. Heckel, J. Mercat, M. Chen, S. Gururangan, M. Wortsman, A. Albalak, Y. Bitton, M. Nezhurina, A. Abbas, C.-Y. Hsieh, D. Ghosh, J. Gardner, M. Kilian, H. Zhang, R. Shao, S. Pratt, S. Sanyal, G. Ilharco, G. Daras, K. Marathe, A. Gokaslan, J. Zhang, K. Chandu, T. Nguyen, I. Vasiljevic, S. Kakade, S. Song, S. Sanghavi, F. Faghri, S. Oh, L. Zettlemoyer, K. Lo, A. El-Nouby, H. Pouransari, A. Toshev, S. Wang, D. Groeneveld, L. Soldaini, P. W. Koh, J. Jitsev, T. Kollar, A. G. Dimakis, Y. Carmon, A. Dave, L. Schmidt, and V. Shankar. Datacomp-Im: In search of the next generation of training sets for language models. *arXiv preprint arXiv:2406.11794*, 2024. 3
- [29] J. Li, D. Li, S. Savarese, and S. Hoi. Blip-2: Bootstrapping language-image pre-training with frozen image encoders and large language models. In *International conference on machine learning*, pages 19730–19742. PMLR, 2023. 11
- [30] J. Li, D. Li, C. Xiong, and S. Hoi. Blip: Bootstrapping language-image pre-training for unified vision-language understanding and generation. In *International conference on machine learning*, pages 12888–12900. PMLR, 2022. 11
- [31] R. Li, L. B. Allal, Y. Zi, N. Muennighoff, D. Kocetkov, C. Mou, M. Marone, C. Akiki, J. Li, J. Chim, Q. Liu, E. Zheltonozhskii, T. Y. Zhuo, T. Wang, O. Dehaene, M. Davaadorj, J. Lamy-Poirier, J. Monteiro, O. Shli-azhko, N. Gontier, N. Meade, A. Zebaze, M.-H. Yee, L. K. Umapathi, J. Zhu, B. Lipkin, M. Oblokulov, Z. Wang, R. Murthy, J. Stillerman, S. S. Patel, D. Abulkhanov, M. Zocca, M. Dey, Z. Zhang, N. Fahmy, U. Bhattacharyya, W. Yu, S. Singh, S. Lucchioni, P. Villegas, M. Kunakov, F. Zhdanov, M. Romero, T. Lee, N. Timor, J. Ding, C. Schlesinger, H. Schoelkopf, J. Ebert, T. Dao, M. Mishra, A. Gu, J. Robinson, C. J. Anderson, B. Dolan-Gavitt, D. Contractor, S. Reddy, D. Fried, D. Bahdanau, Y. Jernite, C. M. Ferrandis, S. Hughes, T. Wolf, A. Guha, L. von Werra, and H. de Vries. Starcoder: may the source be with you! *arXiv preprint arXiv:2305.06161*, 2023. 3
- [32] Y. Li, Y. Du, K. Zhou, J. Wang, W. X. Zhao, and J.-R. Wen. Evaluating object hallucination in large vision-language models. *arXiv preprint arXiv:2305.10355*, 2023. 10
- [33] Y. Li, Y. Zhang, C. Wang, Z. Zhong, Y. Chen, R. Chu, S. Liu, and J. Jia. Mini-gemini: Mining the potential of multi-modality vision language models. *arXiv preprint arXiv:2403.18814*, 2024. 10, 11
- [34] J. Lin, H. Yin, W. Ping, Y. Lu, P. Molchanov, A. Tao, H. Mao, J. Kautz, M. Shoeybi, and S. Han. Vila: On pre-training for visual language models, 2023. 10
- [35] Z. Lin, D. Pathak, B. Li, J. Li, X. Xia, G. Neubig, P. Zhang, and D. Ramanan. Evaluating text-to-visual generation with image-to-text generation. *arXiv preprint arXiv:2404.01291*, 2024. 5, 11
- [36] Z. Lin, D. Pathak, B. Li, J. Li, X. Xia, G. Neubig, P. Zhang, and D. Ramanan. Evaluating text-to-visual generation with image-to-text generation. *arXiv preprint arXiv:2404.01291*, 2024. 5
- [37] H. Liu, C. Li, Y. Li, and Y. J. Lee. Improved baselines with visual instruction tuning. In *Proceedings of the IEEE/CVF Conference on Computer Vision and Pattern Recognition*, pages 26296–26306, 2024. 1, 11
- [38] H. Liu, C. Li, Y. Li, B. Li, Y. Zhang, S. Shen, and Y. J. Lee. Llava-next: Improved reasoning, ocr, and world knowledge, January 2024. 1, 11
- [39] H. Liu, C. Li, Q. Wu, and Y. J. Lee. Visual instruction tuning. *Advances in neural information processing systems*, 36, 2024. 1, 10, 11
- [40] H. Liu, W. Yan, M. Zaharia, and P. Abbeel. World model on million-length video and language with ringattention. *arXiv preprint arXiv:2402.08268*, 2024. 2, 5, 10, 12
- [41] J. Lu, C. Clark, S. Lee, Z. Zhang, S. Khosla, R. Marten, D. Hoiem, and A. Kembhavi. Unified-io 2: Scaling autoregressive multimodal models with vision language audio and action. In *Proceedings of the IEEE/CVF Conference on Computer Vision and Pattern Recognition*, pages 26439–26455, 2024. 10, 12
- [42] Y. Lu, C. Li, H. Liu, J. Yang, J. Gao, and Y. Shen. An empirical study of scaling instruct-tuned large multimodal models. *arXiv preprint arXiv:2309.09958*, 2023. 1, 11
- [43] T. Mihaylov, P. Clark, T. Khot, and A. Sabharwal. Can a suit of armor conduct electricity? a new dataset for open book question answering. *arXiv preprint arXiv:1809.02789*, 2018. 8
- [44] J. Pan, K. Sun, Y. Ge, H. Li, H. Duan, X. Wu, R. Zhang, A. Zhou, Z. Qin, Y. Wang, J. Dai, Y. Qiao, and H. Li. Journeydb: A benchmark for generative image understanding, 2023. 3
- [45] D. Podell, Z. English, K. Lacey, A. Blattmann, T. Dockhorn, J. Müller, J. Penna, and R. Rombach. Sdxl: Improving latent diffusion models for high-resolution image synthesis. *arXiv preprint arXiv:2307.01952*, 2023. 5, 6, 11

- [46] A. Radford, J. W. Kim, C. Hallacy, A. Ramesh, G. Goh, S. Agarwal, G. Sastry, A. Askell, P. Mishkin, J. Clark, et al. Learning transferable visual models from natural language supervision. In *International conference on machine learning*, pages 8748–8763. PMLR, 2021. 1, 11
- [47] A. M. Radhakrishnan. Is midjourney-ai the new anti-hero of architectural imagery & creativity? *GSJ*, 11(1):94–104, 2023. 5, 11
- [48] C. Raffel, N. Shazeer, A. Roberts, K. Lee, S. Narang, M. Matena, Y. Zhou, W. Li, and P. J. Liu. Exploring the limits of transfer learning with a unified text-to-text transformer. *The Journal of Machine Learning Research*, 21(1):5485–5551, 2020. 1
- [49] A. Ramesh, P. Dhariwal, A. Nichol, C. Chu, and M. Chen. Hierarchical text-conditional image generation with clip latents. *arXiv preprint arXiv:2204.06125*, 1(2):3, 2022. 11
- [50] A. Ramesh, M. Pavlov, G. Goh, S. Gray, C. Voss, A. Radford, M. Chen, and I. Sutskever. Zero-shot text-to-image generation. In *International Conference on Machine Learning*, pages 8821–8831. PMLR, 2021. 2, 12
- [51] R. Rombach, A. Blattmann, D. Lorenz, P. Esser, and B. Ommer. High-resolution image synthesis with latent diffusion models. In *Proceedings of the IEEE/CVF conference on computer vision and pattern recognition*, pages 10684–10695, 2022. 5, 6, 11
- [52] K. Sakaguchi, R. L. Bras, C. Bhagavatula, and Y. Choi. Winogrande: An adversarial winograd schema challenge at scale. *Communications of the ACM*, 64(9):99–106, 2021. 8
- [53] M. Sap, H. Rashkin, D. Chen, R. LeBras, and Y. Choi. Socialiqa: Commonsense reasoning about social interactions. *arXiv preprint arXiv:1904.09728*, 2019. 8
- [54] R. Sennrich, B. Haddow, and A. Birch. Neural machine translation of rare words with subword units. In K. Erk and N. A. Smith, editors, *Proceedings of the 54th Annual Meeting of the Association for Computational Linguistics (Volume 1: Long Papers)*, pages 1715–1725, Berlin, Germany, Aug. 2016. Association for Computational Linguistics. 2, 3
- [55] A. Singh, V. Natarajan, M. Shah, Y. Jiang, X. Chen, D. Batra, D. Parikh, and M. Rohrbach. Towards vqa models that can read. In *Proceedings of the IEEE/CVF conference on computer vision and pattern recognition*, pages 8317–8326, 2019. 10
- [56] D. Soboleva, F. Al-Khateeb, R. Myers, J. R. Steeves, J. Hestness, and N. Dey. SlimPajama: A 627B token cleaned and deduplicated version of RedPajama. <https://www.cerebras.net/blog/slimpajama-a-627b-token-cleaned-and-deduplicated-version-of-redpajama>, 2023. 3
- [57] P. Sun, Y. Jiang, S. Chen, S. Zhang, B. Peng, P. Luo, and Z. Yuan. Autoregressive model beats diffusion: Llama for scalable image generation. *arXiv preprint arXiv:2406.06525*, 2024. 2, 12
- [58] Q. Sun, Y. Cui, X. Zhang, F. Zhang, Q. Yu, Y. Wang, Y. Rao, J. Liu, T. Huang, and X. Wang. Generative multimodal models are in-context learners. In *Proceedings of the IEEE/CVF Conference on Computer Vision and Pattern Recognition*, pages 14398–14409, 2024. 1, 11, 12
- [59] Q. Sun, Q. Yu, Y. Cui, F. Zhang, X. Zhang, Y. Wang, H. Gao, J. Liu, T. Huang, and X. Wang. Generative pretraining in multimodality. *arXiv preprint arXiv:2307.05222*, 2023. 1, 10, 11, 12
- [60] C. Team. Chameleon: Mixed-modal early-fusion foundation models. *arXiv preprint arXiv:2405.09818*, 2024. 2, 3, 8, 10, 12
- [61] G. Team, T. Mesnard, C. Hardin, R. Dadashi, S. Bhupatiraju, S. Pathak, L. Sifre, M. Rivière, M. S. Kale, J. Love, et al. Gemma: Open models based on gemini research and technology. *arXiv preprint arXiv:2403.08295*, 2024. 1, 3, 11
- [62] G. Team, M. Rivière, S. Pathak, P. G. Sessa, C. Hardin, S. Bhupatiraju, L. Hussenot, T. Mesnard, B. Shahriari, A. Ramé, et al. Gemma 2: Improving open language models at a practical size. *arXiv preprint arXiv:2408.00118*, 2024. 3
- [63] K. Tian, Y. Jiang, Z. Yuan, B. Peng, and L. Wang. Visual autoregressive modeling: Scalable image generation via next-scale prediction. *arXiv preprint arXiv:2404.02905*, 2024. 2, 12
- [64] H. Touvron, T. Lavril, G. Izacard, X. Martinet, M.-A. Lachaux, T. Lacroix, B. Rozière, N. Goyal, E. Hambro, F. Azhar, et al. Llama: Open and efficient foundation language models. *arXiv preprint arXiv:2302.13971*, 2023. 1, 11
- [65] H. Touvron, L. Martin, K. Stone, P. Albert, A. Almahairi, Y. Babaei, N. Bashlykov, S. Batra, P. Bhargava, S. Bhosale, et al. Llama 2: Open foundation and fine-tuned chat models. *arXiv preprint arXiv:2307.09288*, 2023. 1, 8, 11
- [66] A. Van Den Oord, O. Vinyals, et al. Neural discrete representation learning. *Advances in neural information processing systems*, 30, 2017. 2
- [67] X. Wang, X. Zhang, Z. Luo, Q. Sun, Y. Cui, J. Wang, F. Zhang, Y. Wang, Z. Li, Q. Yu, et al. Emu3: Next-token prediction is all you need. *arXiv preprint arXiv:2409.18869*, 2024. 2
- [68] Y. Wang, T. Xiong, D. Zhou, Z. Lin, Y. Zhao, B. Kang, J. Feng, and X. Liu. Loong: Generating minute-level long videos with autoregressive language models. *arXiv preprint arXiv:2410.02757*, 2024. 11
- [69] C. Wu, X. Chen, Z. Wu, Y. Ma, X. Liu, Z. Pan, W. Liu, Z. Xie, X. Yu, C. Ruan, et al. Janus: Decoupling visual encoding for unified multimodal understanding and generation. *arXiv preprint arXiv:2410.13848*, 2024. 5, 12

- [70] Y. Wu, Z. Zhang, J. Chen, H. Tang, D. Li, Y. Fang, L. Zhu, E. Xie, H. Yin, L. Yi, et al. Vila-u: a unified foundation model integrating visual understanding and generation. *arXiv preprint arXiv:2409.04429*, 2024. [2](#), [5](#), [10](#), [12](#)
- [71] J. Xie, W. Mao, Z. Bai, D. J. Zhang, W. Wang, K. Q. Lin, Y. Gu, Z. Chen, Z. Yang, and M. Z. Shou. Show-o: One single transformer to unify multimodal understanding and generation. *arXiv preprint arXiv:2408.12528*, 2024. [2](#), [5](#), [10](#), [12](#)
- [72] J. Yu, Y. Xu, J. Y. Koh, T. Luong, G. Baid, Z. Wang, V. Vasudevan, A. Ku, Y. Yang, B. K. Ayan, et al. Scaling autoregressive models for content-rich text-to-image generation. *arXiv preprint arXiv:2206.10789*, 2(3):5, 2022. [2](#), [12](#)
- [73] L. Yu, B. Shi, R. Pasunuru, B. Muller, O. Golovneva, T. Wang, A. Babu, B. Tang, B. Karrer, S. Sheynin, et al. Scaling autoregressive multi-modal models: Pretraining and instruction tuning. *arXiv preprint arXiv:2309.02591*, 2(3), 2023. [10](#)
- [74] R. Zellers, A. Holtzman, Y. Bisk, A. Farhadi, and Y. Choi. Hellaswag: Can a machine really finish your sentence? *arXiv preprint arXiv:1905.07830*, 2019. [8](#)
- [75] L. Zheng, W.-L. Chiang, Y. Sheng, T. Li, S. Zhuang, Z. Wu, Y. Zhuang, Z. Li, Z. Lin, E. P. Xing, et al. Lmsys-chat-1m: A large-scale real-world llm conversation dataset. *arXiv preprint arXiv:2309.11998*, 2023. [10](#)
- [76] C. Zhou, L. Yu, A. Babu, K. Tirumala, M. Yasunaga, L. Shamis, J. Kahn, X. Ma, L. Zettlemoyer, and O. Levy. Transfusion: Predict the next token and diffuse images with one multi-modal model. *arXiv preprint arXiv:2408.11039*, 2024. [2](#)
- [77] D. Zhu, J. Chen, X. Shen, X. Li, and M. Elhoseiny. Minigpt-4: Enhancing vision-language understanding with advanced large language models. *arXiv preprint arXiv:2304.10592*, 2023. [1](#), [11](#)